Astronomy & Astrophysics

LETTER TO THE EDITOR

Shocked water in the Cepheus E protostellar outflow

B. Lefloch[1,2], J. Cernicharo[2], S. Pacheco[1], and C. Ceccarelli[1]

[1] UJF-Grenoble 1/CNRS-INSU, Institut de Planétologie et d'Astrophysique de Grenoble (IPAG) UMR 5274, Grenoble 38041, France
e-mail: lefloch@obs.ujf-grenoble.fr

[2] Laboratorio de Astrofísica Molecular, Departamento de Astrofísica, Centro de Astrobiologia, INTA, Ctra de Torrejón a Ajalvir, km 4, 28850 Torrejón de Ardoz, 28850 Madrid, Spain

ABSTRACT

Context. Previous far-infrared observations at low-angular resolution have reported the presence of water associated with low-velocity outflow shocks and protostellar envelopes.
Aims. We want to elucidate the origin of water emission in protostellar systems.
Methods. The outflow driven by the intermediate-mass class 0 protostar Cep E is among the most luminous outflows detected so far. Using the IRAM 30 m telescope, we searched for and detected the p-H_2O $3_{13}-2_{20}$ line emission at 183 GHz in the Cep E star-forming core. The emission arises from high-velocity gas close to the protostar, which is unresolved in the main beam of the telescope. Complementary observations at 2″ resolution with the Plateau de Bure interferometer helped establish the origin of the emission detected and the physical conditions in the emitting gas. The water line profile and its spatial distribution are very similar to those of SiO. We find that the H_2O emission arises from warm ($\sim$200 K), dense (($1-2$) $\times 10^6$ cm^{-3}) gas, and its abundance is enhanced by one to two orders of magnitude with respect to the protostellar envelope.
Results. We detect water emission in strong shocks from the high-velocity jet at 1000 AU from the protostar. Despite the large beam size of the telescope, such emission should be detectable with Herschel.

Key words. stars: formation – ISM: molecules – ISM: jets and outflows – ISM: individual objects: Cep E

1. Introduction

Water is a key molecule not only for oxygen chemistry in the interstellar gas, but also in the dynamical evolution of star-forming regions, because it is one of the main gas coolants (Kaufman & Neufeld 1996; Bergin et al. 1998). Whereas its abundance is very low in dark clouds, prestellar cores, and starless regions (from less than 10^{-8} to a few 10^{-7}; Bergin & Snell 2002; Moneti et al. 2001), it can be greatly enhanced in star-forming regions, through the sputtering of frozen water from grain mantles and through high-temperature, sensitive reactions in the gas phase (Elitzur & de Jong 1978; Ceccarelli et al. 1996; Kaufmann & Neufeld 1996). It has been proposed that such processes are driven by the heating of the nascent stars (hot core/corino region) or by shocks either in the accretion region in the inner protostellar core or in the outflow carrying away the angular momentum of the envelope. Previous observations of water lines obtained with the *Infrared Space Observatory* have substantially confirmed these theoretical expectations (see e.g. Giannini et al. 2001; Ceccarelli et al. 2000; van Dishoeck 2004, for a review). However, many details are still missing and the relative efficiency of these mechanisms is not known, so that the origin of the water emission in protostellar regions remains a puzzle to be solved. One obstacle is indeed the relatively low spatial resolution of these observations.

Most of the H_2O lines cannot be observed from ground because of strong atmospheric absorption. The para-H_2O line $3_{13}-2_{20}$ at 183.3 GHz is an exception since it can be enhanced by the masing effect even in regions of moderate excitations. Using the IRAM 30 m telescope, Cernicharo et al. (1990, 1994)

detected large-scale p-H_2O $3_{13}-2_{20}$ line emission in giant molecular clouds and star-forming regions and they showed that this line can be used to investigate the spatial distribution of H_2O in protostellar environments at an angular resolution comparable to the size of the protostellar cores (14″ at the IRAM 30 m telescope). Observing the low-mass protostellar outflows HH 7-11 and L1448, Cernicharo et al. (1996) detected water line emission arising from shocks associated with the Herbig-Haro objects in the outflows.

In this Letter, we report on observations of the p-H_2O $3_{13}-2_{20}$ line in the star-forming core Cep E with the IRAM 30 m telescope[1]. Located at 730 pc, it is a relatively nearby intermediate-mass Class 0 source of 100 $L_\odot$ and a mass of 18 $M_\odot$, intensively studied at mm and IR wavelengths (Moro-Martin et al. 2001; Noriega-Crespo et al. 2004; Lefloch et al. 1996, hereafter L96). The protostar drives an exceptionally powerful outflow, whose southern lobe is terminated by the Herbig-Haro object HH 377. Far-infrared observations at low spectral and angular resolution with ISO have revealed large amounts of water, which Giannini et al. (2001) interpret as arising from low-velocity shocks, whose far-infrared luminosity amounts to $L \sim 3$ $L_\odot$.

Observations of the millimeter lines of SiO observations reveal the presence of strong shocks along the outflow (L96). Because it is usually undetected in the cold, quiescent molecular gas, SiO is a particularly good tracer of shocks that are strong enough to release refractory elements from grain cores. Recent

Herschel observations suggest that SiO is also a good tracer of the water-emitting shock regions (Lefloch et al. 2010; Nisini et al. 2010). We present observations of the high-excitation SiO $J = 8 \rightarrow 7$ line towards the protostar.

2. Observations

2.1. Water observation

We observed the line of para-H_2O $3_{13} \rightarrow 2_{20}$ at 183.3 GHz at the IRAM 30 m telescope in January 2009, near the transit of Cep E between 61° and 65° of elevation. Both receivers at 2 mm were used simultaneously. Observations were carried out in wobbler switching mode with a throw of 180″. Filterbanks with 1 MHz spectral resolution and an autocorrelator providing a spectral resolution of 1.25 MHz (2 km s⁻¹) were used as spectrometers. Weather conditions were very good and stable, with an atmospheric optical depth ≈1.10 along the line of sight. Calibration was carefully monitored every 4 minutes between two integration scans on Cep E. Water vapor and system temperatures were found to remain stable, in the range 1650−1800 K. Any fluctuation of the sky emissivity between the on and off positions would result in a poor spectroscopic baseline and detection of the mesospheric water line, which is not the case in the present observations. Pointing was checked against nearby quasars every hour and has an accuracy of ≈2″. At the frequency of the H_2O line, the main-beam efficiency of the telescope is 0.63 and the half-power beamwidth is 13.2″. We did a small oversampled map at 6″ sampling of the southern lobe of the outflow, centered on the nominal position of the protostar $23^h03^m13.0^s$ +61°42′21″ (J2000). The typical rms is 100 mK per velocity interval of 2 km s⁻¹.

2.2. SiO observations

The SiO $J = 8 \rightarrow 7$ transition at 347.33006 GHz was observed towards the protostar at the JCMT in August 2005. The weather conditions were good with an average system temperature $T_{sys} \sim$ 400 K. Observations were carried out with a nutating secondary, adopting a throw of 60″. The DBS was used as spectrometer, providing a spectral resolution of 625 kHz. The resolution was degraded to 3.75 MHz, corresponding to a final velocity resolution of about 3.2 km s⁻¹. At the frequency of the SiO line, the main-beam efficiency of the telescope is about 0.60 and the half-power beamwidth is ≃14.2″, very similar to the telescope parameters of the p-H_2O observations. Complementary interferometric observations at 2″ resolution with the Plateau de Bure in the SiO $J = 2 \rightarrow 1$ transition provide us with the spatial distribution of the emission and its excitation conditions. These observations will be presented and discussed in detail in a forthcoming paper (Lefloch et al., in prep.).

3. Results and discussion

3.1. Water emission in Cep E

The map of the p-H_2O $3_{13}−2_{20}$ emission in Cep E is displayed in the left panel of Fig. 1. Emission is detected only towards the protostellar core, in a region unresolved by the main beam of the IRAM 30 m telescope. In particular, we do not detect any H_2O emission towards HH77, the southern bowshock at offset position (−5″, −15″), associated with bright emission in the lines of SiO and H_2 (L96). To improve the signal-to-noise ratio of the data, we averaged the emission of the water line over the inner
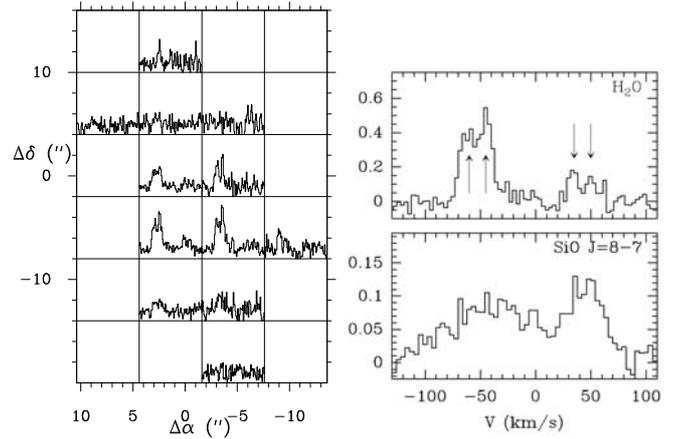
Fig. 1. (*Left*) Map of the p-H_2O $3_{13}−2_{20}$ emission between −110 and +70 km s⁻¹ in the outflow of Cep E obtained with the IRAM 30 m telescope. Coordinates are in arcsec offsets with respect to the nominal position of the protostar. (*Right*) H_2O and SiO $J = 8 \rightarrow 7$ emission detected towards the protostellar source. The H_2O emission is averaged over a region of 6″ × 6″ around the protostar. Intensities are expressed in units of antenna temperature. The different components of the spectrum are marked with arrows.

core, in the range $\Delta\alpha = [1″; −5″]$ $\Delta\delta = [1″; −5″]$. The averaged spectrum is displayed in the right panel of Fig. 1, and the final rms noise is 30 mK (T_A^*) per interval of 2 km s⁻¹.

Two bright components (∼1 K) with broad linewidths (∼10 km s⁻¹) are detected at about $v_{lsr} \approx −65$ and $−45$ km s⁻¹ in the direction of the protostar. Two other, weaker, H_2O components are detected at approximately symmetric (redshifted) velocities $v_{lsr} \approx +34$ and $+50$ km s⁻¹. We do not detect any emission at the velocity of the protostellar envelope ($v_{lsr} = −10.9$ km s⁻¹; L96), hence excluding any contribution from the hot corino to the water emission. The presence of both blue- and redshifted components in the water line spectrum indicates that the emission arises from the central protostellar region. This is because there is barely any overlap in the plane of the sky between the blue and redshifted wings of the Cep E outflow, except in the central protostellar region as a consequence of the limited angular resolution of the observations (see Figs. 1, 2; also L96).

The spectrum of the SiO $J = 8 \rightarrow 7$ emission in the direction of the protostar is displayed in Fig. 1 and looks very similar to the p-H_2O $3_{13}−2_{20}$ line spectrum. Resemblance between both emissions is even more striking when comparing the water spectrum with the $J = 2 \rightarrow 1$ emission observed with the PdBI (Fig. 2). This suggests that the emission of both tracers arises from the same region. Observations of the $J = 2 \rightarrow 1$ transition with the PdBI of the central protostellar regions (Lefloch et al., in prep.) show that the SiO emission arises from two compact clumps, in the blue- and redshifted gas, respectively, located at ≈1.5″ from the protostar. They have a typical size of 2.5″ (2.3×10^{16} cm), and a transverse size of 1″ (Fig. 2). Their similar physical properties (size, velocity, distance) suggest they are related to an episodic ejection phenomenon. In what follows, we assume that both the H_2O and the SiO emissions have the same size.

3.2. Physical conditions

The gas kinetic temperature T_k in the redshifted, high-velocity jet was previously determined by Hatchell et al. (1999) from JCMT observations of the CO $J = 4 \rightarrow 3$ and $J = 2 \rightarrow 1$ lines.
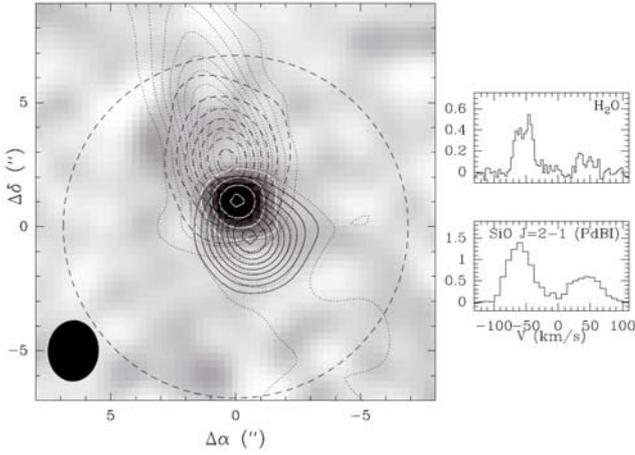
Fig. 2. (*Left*) Map of the velocity-integrated SiO emission in the Cep E jet obtained at $2''$ resolution with the Plateau de Bure interferometer (PdBI; Lefloch et al., in prep.). The SiO $J = 2 \rightarrow 1$ emission integrated between $+40$ and $+80$ km s^{-1} (-90 and -40 km s^{-1}) is drawn in solid (dashed) contours, superposed on the 3 mm continuum emission map (grayscale and white contours). First contour and contour interval of the jet emission are 10^{-2} and 5×10^{-3} (10^{-2}) Jy/beam for the redshifted (blueshifted) emission. First contour and contour interval of the 3 mm continuum emission is 2×10^{-3} Jy/beam. The main beam of the IRAM 30 m telescope at the frequency of the p-H$_2$O $3_{13}-2_{20}$ line is marked by a circle (dashed). The synthesized beam of the PdBI ($2.4'' \times 2.0''$) is indicated as a filled ellipse in the bottom right corner. (*Right*) Comparison of the PdBI SiO $J = 2 \rightarrow 1$ and the average p-H$_2$O $3_{13}-2_{20}$ spectra towards the protostar. Intensities are expressed in units of antenna temperature.
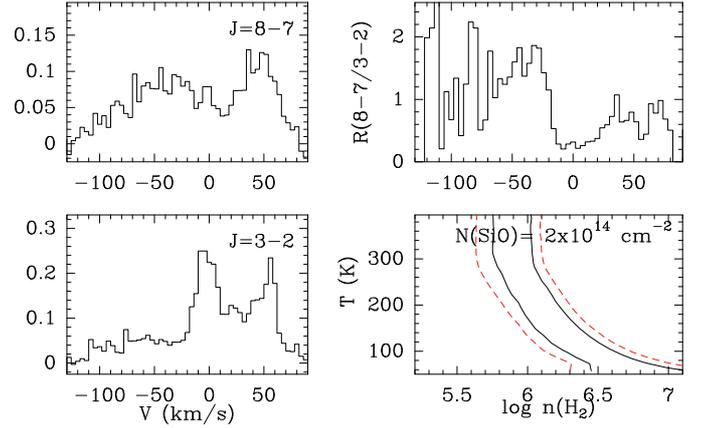

Fig. 3. (*Left*) SiO emission observed in the $J = 3 \rightarrow 2$ (*bottom*) and $J = 8 \rightarrow 7$ transitions towards the protostellar source. Fluxes are expressed in units of main-beam temperature. (*Right*) Observed variations of the ratio of the CO $J = 8 \rightarrow 7$ to $J = 3 \rightarrow 2$ brigthness temperatures $R(8-7/3-2)$ as a function of velocity (top) and predicted variations as a function of the gas density $n(H_2)$ and the kinetic temperature T_k (bottom) for a typical column density $N(SiO) = 2 \times 10^{14}$ cm^{-2}. The contour level $R = 0.7, 1.5$ are drawn with a solid black line; the contours $R = 0.5, 1.8$ are drawn with a dashed red line and account for an uncertainty of 30%.

Unfortunately, their analysis is biased by a highly overestimated value of the main-beam efficiency η_{MB} of the $J = 4 \rightarrow 3$ observations, poorly known at that time, leading to an underestimate of T_k ($\approx$50 K). Based on their observations and adopting a standard value consistent with the subsequent determinations from point-like calibrators[2], $\eta_{MB} = 0.35$, we obtain the jet kinetic temperature and column density, $T_k \simeq 120$ K and $N(CO) \simeq 2.5 \times 10^{17}$ cm^{-2}, respectively (see also L96). Adopting a standard CO abundance in the gas, we then derive the source-averaged gas column-density $N(H_2) \simeq 2.5 \times 10^{21}$ cm^{-2}. We adopt these values of T_k and N(CO) for both water-emitting clumps at blue- and redshifted velocities.

The gas density and column density in the water-emitting clumps were derived from modeling the H$_2$O and SiO line brightness temperatures in the large-velocity gradient (LVG) approach. We adopted the collisional coefficients of Faure et al. (2007) and Dayou & Balança (2006), respectively. The gas density can be constrained reasonably well from the ratio of the SiO $J = 8 \rightarrow 7$ to $J = 3 \rightarrow 2$ brightness temperatures. This ratio was computed using the SiO $J = 3 \rightarrow 2$ observations in the Cep E protostellar core obtained by L96 (see also Fig. 3). We note that the source is unresolved by the single-dish JCMT and IRAM 30 m observations; therefore, we approximated the ratio of the line brightness temperatures by the ratio of the main-beam brightness temperatures corrected for the difference of main-beam solid angles $R(8-7/3-2)$. A description of the radiative transfer code and the procedure applied to deal with the masing effect is presented in Cernicharo et al. (1994) and González-Alfonso & Cernicharo (1993).

The top right panel of Fig. 3 displays the variations of $R(8-7/3-2)$. The ratio varies little in the low-velocity gas and is about 0.2. It increases as a function of velocity and reaches values up to 0.7 and 1.5 in the redshifted and blueshifted gas, respectively. The variations of $R(8-7/3-2)$ as a function of T_k and $n(H_2)$ were computed for a typical column density $N(SiO) = 2 \times 10^{14}$ cm^{-2} and a linewidth $\Delta V = 10$ km s^{-1}, and they are displayed in Fig. 3. With the constraint $T_k \geq 100$ K, it comes out that $n(H_2)$ must be about 1.0×10^6 cm^{-3} in order to account for the line intensity ratio in the redshifted gas. The density in the blueshifted gas is slightly higher $\approx 2 \times 10^6$ cm^{-3}. These calculations show that the ratio depends weakly on T_k above 100 K. For these values of $n(H_2)$ and the kinetic temperature estimated above, we estimate the source-averaged column density necessary to account for the $J = 8 \rightarrow 7$ line intensity $N(SiO) = (2.0-3.3) \times 10^{14}$ cm^{-2} for gas at 120 K in the blue- and redshifted components. Under such physical conditions both SiO transitions are optically thin, so that $R(8-7/3-2)$ depends weakly on the adopted value of the gas column density. From comparison with $N(CO)$ and assuming a standard abundance [CO]/[H$_2$] = 10^{-4}, we obtain the relative SiO abundance in the shock: [SiO]/[H$_2$] $\simeq 1.0 \times 10^{-7}$, similar to the abundances measured in other Class 0 protostellar outflows (Lefloch et al. 1998).

The para-water (source-averaged) column density $N(p-H_2O)$ was determined from modeling the line brightness temperature T_B. The latter was derived from the main-beam brightness temperature $T_{MB} = T_B \times ff$, where the filling factor ff was obtained assuming that the H$_2$O and SiO $J = 2 \rightarrow 1$ emitting regions have similar sizes, in agreement with Sect. 3.1. We find $T_B = 60-80$ K and $15-29$ K in the blueshifted and redshifted gas, respectively. The brightness temperature of the p-H$_2$O $3_{13}-2_{20}$ line was computed for a wide range of physical conditions, adopting a typical linewidth $\Delta v = 10$ km s^{-1} : T_k between 50 and 200 K, $n(H_2)$ in the range 10^3-10^8 cm^{-3} and $N(p-H_2O)$ in the range 3×10^{16} to 10^{19} cm^{-2}. The results of the calculations are presented in Fig. 4.
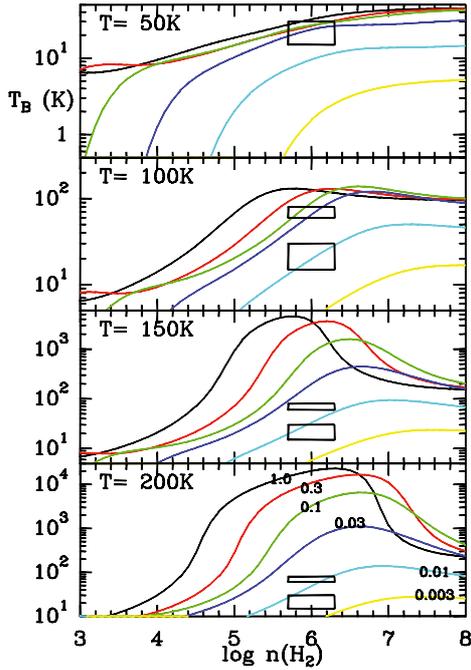
Fig. 4. Predictions of the p-H_2O $3_{13}-2_{20}$ line intensity, in units of brightness temperature, for gas with density $n(H_2)$ in the range 10^3-10^8 cm^{-3}, temperature in the range $50-200$ K, for column densities of para-water equal to 0.003 (*bottom curve*), 0.01, 0.03, 0.1, 0.3, 1.0×10^{19} cm^{-2} (*top curve*). The range of $T_B-n(H_2)$ determined in the water-emitting clumps is delineated by rectangles.

It comes out that the kinetic temperature T_k has to be higher than 100 K to account for brightness temperatures of $60-80$ K. Our calculations indicate a p-H_2O column density in the range $(0.3-2.0) \times 10^{17}$ cm^{-2} for $T_k \simeq 200$ K. Assuming an ortho-to-para ratio of 3, we derive $N(H_2O) = (1.2-8.0) \times 10^{17}$ cm^{-2}, and using the H_2 column density derived in the high-velocity clumps, we obtain the water abundance $X(H_2O) = (0.5-3.2) \times 10^{-4}$. In this range of physical conditions, the line optical depth τ is small ≈-1 and shows evidence for the weak masing amplification of p-H_2O $3_{13}-2_{20}$ line. Suprathermal excitation of the line would require much higher H_2O column densities. This is possible if the emission arises from a small region of subarsec size (see e.g. Cernicharo et al. 1994) and is very sharp. The line T_B would then look weaker as a result of the dilution in the 2 km s^{-1} channels of the spectrometer.

Moro-Martin et al. (2001) analyzed the far-infrared emission lines of CO and H_2O in Cep E, as observed with ISO. Like Giannini et al. (2001), they found that the line emission can be accounted for by an extended component of low-density gas (2×10^4 cm^{-3}) at $\sim$1000 K. They show that the CO and H_2O lines could be reproduced equally well by "warm" gas at a much lower temperature ($\sim$200 K) and higher density (2×10^6 cm^{-3}). The physical conditions we derive for the p-H_2O $3_{13}-2_{20}$ emitting region are actually in rather good agreement with this "warm" solution and inconsistent with the low-density "hot" solution.

3.3. Shocked water in Cep E

Crimier et al. (2010) determined the physical conditions in the protostellar envelope of Cep E envelope and found $n(H_2) = 1.0 \times 10^7$ cm^{-3} and $T_k \sim 50$ K, respectively, at the location of the water-emitting clumps, i.e. 1000 AU (1.4″) from the protostar. No p-H_2O $3_{13}-2_{20}$ emission is detected from the envelopeat the 2σ level = 3 K (T_B). From Fig. 4, we conclude that $N(H_2O) < 10^{16}$ cm^{-2} in the inner protostellar envelope, and the water abundance is enhanced by 1 to 2 orders of magnitude in the high-velocity clumps. The authors estimate a radius of $\approx$220 AU(0.3″) for the hot corino region, and the density is predicted very high $\sim$10^8 cm^{-3}; again, no masing effect is to be expected, in agreement with our observations.

The water-emitting clumps are located along the high-velocity jet, which suggests that they are closely related with the jet (Fig. 2). One possibility is that these clumps are tracing the jet/envelope interaction. However, the density of the protostellar envelope, as estimated by Crimier et al. (2010) at the location of the water emitting-clumps ($n(H_2) = 1.0 \times 10^7$ cm^{-3}), is about one order of magnitude higher than the density measured in the shocked gas (10^6 cm^{-3}), in apparent contradiction with this hypothesis. The structure of the envelope could be actually more complex than the simple power-law distribution derived by Crimier et al. (2010), as proposed that multiple protostars are embedded inside the core (Ladd & Hodapp 1997). Direct observational evidence for several condensations is still missing, however. Alternatively, we speculate that the water emission could arise from internal shocks in the entrained material of the flow. Interferometric observations at subarcsec scale in the inner core ($r < 1000$ AU) are needed to determine the gas density and velocity field in order to determine the location and the origin of the water-emitting shocks, as well as their relation with the jet.

Simple calculations in the LVG approximation predict that the H_2O emission from the high-velocity clumps should be easily detected in several ortho- and para-H_2O transitions with the high-resolution spectrometer HIFI onboard *Herschel*. Such observations will allow us to better constrain the shock physical conditions (see e.g. Flower & Pineau des Forets 2010).

References

Bergin, E. A., & Snell, R. L. 2002, ApJ, 581, L105
Bergin, E. A., Neufeld, D. A., & Melnick, G. J. 1998, ApJ, 499, 777
Ceccarelli, C., Hollenbach, D., & Tielenas, A. G. G. M. 1996, ApJ, 471, 400
Ceccarelli, C., Castets, A., Caux, E., et al. 2000, ApJ, 355, 1129
Cernicharo, J., Thum, C., Hein, H., et al., A&A, 1990, 231, L15
Cernicharo, J., Gonzalez-Alfonso, E., & Alcolea, J. 1994, 432, L59
Cernicharo, J., Bachiller, R., & Gonzalez-Alfonso, E. 1996, A&A, 305, L5
Crimier, N., Ceccarelli, C., & Alonso-Albi, T., et al. 2010, A&A, 516, A102
Dayou, F., & Balança, C. 2006, A&A, 459, 297
Eisloeffel, J., Smith, M. D., & Davis, C.J. 1996, AJ, 112, 2086
Elitzur, M., & de Jong, T., 1978, A&A, 67, 323
Faure, A., Crimier, N., Ceccarelli, C., et al. 2007, A&A, 472, 1029
Flower, D. R., & Pineau des Forets, G. 2010, MNRAS, 406, 1745
Giannini, T., Nisini, B., & Lorenzetti, D. 2001, ApJ, 555, 40
Kaufman, M., & Neufeld, D. 1996, ApJ, 456, 611
Ladd, E. F., & Hodapp, K.-W. 1997, ApJ, 475, 749
Lefloch, B., Eisloeffel, J., & Lazareff, B. 1996, A&A, 313, L17 (L96)
Lefloch, B., Castets A., Cernicharo, J., et al. 1998, A&A, 504, L109
Moneti, A., Cernicharo J., & Pardo J. R. 2001, ApJ, 549, L203
Moro-Martín, A., Noriega-Crespo, A., Molinari, S., et al., 2001, ApJ, 555, 146
Nisini, B., Benedettini, M., Codella, C. et al. 2010, A&A, 518, L120
Noriega-Crespo, A., Moro-Martin, A., & Carey, S. 2004, ApJS, 154, 402
Turner, B. E., Chan, Kin-Wing, Green, S., et al. 1992, ApJ, 399, 114
van Dishoeck, E. F. 2004, ARA&A, 42, 119